PFC/JA-95-5

Theory of Low Mach Number Compressible Flow

A. Shajii and J.P. Freidberg

February 1995

Plasma Fusion Center
Massachusetts Institute of Technology
Cambridge, MA 02139 USA

Submitted for publication in: **Journal of Fluid Mechanics**

This work was supported by the US Department of Energy under contract DE-FG-02-91-ER54110. Reproduction, translation, publication, use, and disposal, in whole or in part, by or for the US Government is permitted.

Abstract

The properties of a relatively uncommon regime of fluid dynamics, low Mach number compressible flow are investigated. This regime, which is characterized by an exceptionally large tube aspect ratio $L/d \sim 10^6$ leads to highly subsonic flows in which friction dominates inertia. Even so, because of the large aspect ratio, finite pressure, temperature, and density gradients are required, implying that compressibility effects are also important. Analytic results are presented for both the laminar and turbulent regimes. Perhaps the most interesting result is that in forced flow situations steady state solutions exist only below a critical value of heat input. Above this value the flow reverses against the direction of the applied pressure gradient causing fluid to leave both the inlet and outlet implying that the related concepts of a steady state friction factor and heat transfer coefficient have no validity.

I. Introduction

This paper describes the basic properties of a relatively uncommon regime of fluid dynamics, low Mach number compressible flow (LMCF). Such flows have distinctly different behavior than the more familiar and extensively investigated regimes of high Mach number compressible flow (of great interest to aerodynamicist) and low Mach number incompressible flow (of great interest to many mechanical engineering applications).

The motivation to study the LMCF regime results from research [1,2] on the cooling of large scale superconducting magnets such as might be used in next generation magnetic fusion experiments [3]. A typical magnet coil has dimensions on the order of 20 m $\times$ 8 m $\times$ 1 m. Because of the need for electrical continuity of the superconductor each coil is fabricated from a single, uninterrupted length of cable $L \approx 1$ km. The cross section of the cable is circular with a radius $R_c \approx 2$ cm. The cable itself is comprised of approximately 1000 tightly compacted, twisted superconducting/copper strands, each strand having a radius $R_s \approx 0.5$ mm. The coil is cooled by supercritical helium flowing between the strands. With regard to the fluid dynamic behavior of the coolant, the geometry implies that the hydraulic diameter for the flow is comparable to the strand diameter: $d \approx 1$ mm. Consequently, the aspect ratio of the flow has the enormous value $L/d \approx 10^6$.

This is the crucial property of LMCF. With such a large aspect ratio, the flow is dominated by friction rather than inertia. The resulting flows are highly subsonic: $M \sim 0.02$. Even so, because of the long lengths involved, a finite pressure gradient is required to drive the flow. Thus, the usual equivalence of low Mach number and incompressible flow [4] does not apply; that is, even though $M \ll 1$, the finite gradients in p, ρ, and T imply that compressibility is an important effect that must be included in the modelling.

Of the many areas of fluid dynamics that have been studied, the one that most nearly resembles LMCF is that of gaseous flow through a porous media [5]. Here, too, the flows are subsonic and compressibility must be included. However, in the investigations thus far presented (mainly corresponding to flow in capillary tubes) the ratio L/d while large, is not so large that finite pressure gradients are required [5,6]. The compressibility could thus be treated perturbatively about an incompressible state, with $\Delta p/p$ being the expansion

parameter [7,8]. Even with small compressibility it was shown that important modifications arise in the laminar pressure and velocity profiles [7-9].

The work described here assumes $M \ll 1$ and $\Delta p/p \sim \Delta T/T \sim \Delta \rho/\rho \sim 1$. As an initial attempt to understand the flow properties of the LMCF regime we focus on the problem of steady state flow of an ideal gas in a tube. Both laminar and turbulent conditions are considered. The goals are to (1) determine the basic flow and heat removal properties of the gas, (2) develop an understanding of equivalent friction factor and heat transfer coefficient and how they might be measured experimentally in the laminar regime, and (3) develop insight into the effects of turbulence on the flow. A number of new and somewhat surprising results follow from the analysis and are summarized below.

1. A basic LMCF ordering is defined from which we derive the nonlinear, time dependent LMCF model.

2. Analytic solutions are obtained for the flow properties in the case $\mu =$ const. and $\kappa =$ const. (here μ is the viscosity and κ is the thermal conductivity).

3. The analytic solutions are generalized to the more realistic case $\mu = \mu(T)$ and $\kappa = \kappa(T)$. In this situation there exist two bifurcated solutions, only one of which is stable.

4. It is demonstrated that experimental measurements of the friction factor f and heat transfer coefficient h are coupled. For instance to determine f, not only are the flow rate and pressure drop required, but one must also measure the inlet and outlet temperatures and the applied heat flux. A similar consideration applies to h.

5. Somewhat surprisingly, for a given pressure drop Δp, steady state solutions (and the corresponding concepts of a steady state friction factor and heat transfer coefficient) exist only when the applied heat flux lies below a critical value: $q < q_c$. For $q > q_c$, the flow never reaches steady state. Instead, at some point in the tube, the flow reverses against the applied pressure gradient. Fluid then flows out of both the inlet and outlet quickly depleting the system of coolant.

6. For the more realistic case $\mu = \mu(T)$, $\kappa = \kappa(T)$, it is shown that in conjunction to the condition $q < q_c$, there is an additional requirement that the mass flow satisfy

$\dot{m} > \dot{m}_c$. Attempts to measure f and h at low flow rates again lead to flow reversal and depletion of the helium.

7. The effects of turbulence are modelled by introducing a friction factor in place of the laminar viscosity. The qualitative nature of the flow remains unchanged although the value of q_c is reduced relative to its laminar value as the Reynolds number is increased.

The analysis leading to these conclusions is described in the main body of the text.

II. Model

The starting point for the analysis is the set of general mass, momentum, and energy conservation laws for an ideal, compressible, monotonic gas. The corresponding equations are given by [10]

$$\frac{\partial \rho}{\partial t} + \nabla \cdot \rho \mathbf{v} = 0 \tag{1}$$

$$\rho \left(\frac{\partial \mathbf{v}}{\partial t} + \mathbf{v} \cdot \nabla \mathbf{v} \right) = -\nabla p - \nabla \cdot \overleftrightarrow{\tau} \tag{2}$$

$$\rho C_v \left(\frac{\partial T}{\partial t} + \mathbf{v} \cdot \nabla T \right) + \rho C_\beta T \nabla \cdot \mathbf{v} = -\nabla \cdot \mathbf{q} - \overleftrightarrow{\tau} : \nabla \mathbf{v} \tag{3}$$

$$p = R \rho T \tag{4}$$

For the gas under consideration $C_v = (3/2)R$ and $C_\beta = R$. The stress tensor and heat flux have their usual forms

$$\overleftrightarrow{\tau} = -\mu \left[\nabla \mathbf{v} + (\nabla \mathbf{v})^T \right] + \frac{2}{3} \mu (\nabla \cdot \mathbf{v}) \overleftrightarrow{\mathbf{I}}$$

$$\mathbf{q} = -\kappa \nabla T$$

where $\overleftrightarrow{\mathbf{I}}$ is the identity tensor and μ and κ are assumed to be functions of T.

Consider the regime of low Mach number, compressible flow (LMCF) a situation that arises when the length of a tube L is sufficiently large with respect to its hydraulic diameter d. In this regime the frictional force due to viscosity dominates inertial effects, leading to a

low Mach number flow even though the pressure gradient is finite. The practical conditions under which this occurs correspond to

$$v \sim \frac{pd^2}{\mu L} \ll v_s \tag{5a}$$

or equivalently

$$M^2 \sim \frac{d}{L} Re \ll 1 \tag{5b}$$

where $M = v/v_s$ is the Mach number and $Re = \rho v d/\mu$ is the Reynolds number. Note that we are concerned with flow gradients occurring over the entire length of the tube L. A different scaling would be required for short scale entrance problems.

When Eq. (5) is satisfied the basic model can be easily recast in a dimensionless form containing only three dimensionless parameters, M^2, (d/L), and the Prandtl number $Pr = C_p \mu/\kappa$ which is always on the order of unity for gases. Based on the above discussion one can now introduce a basic ordering scheme that defines low Mach number, compressible flow

$$v_\perp/v_z \sim d/L \sim (\partial/\partial z)/\nabla_\perp \sim M^2 \sim \epsilon \ll 1 \tag{6a}$$

$$(L/v_z)\partial/\partial t \sim \frac{\mu L v_z}{pd^2} \sim \frac{\Delta p}{p} \sim \frac{\Delta T}{T} \sim \frac{\Delta \rho}{\rho} \sim Pr \sim 1. \tag{6b}$$

Here Δp, ΔT, $\Delta \rho$ are the changes in p, T, ρ from inlet to outlet, and the subscripts z and $\perp$ refer to the parallel and transverse flow directions respectively. For convenience ϵ has been introduced as a formal ordering parameter.

As a reference case, consider a small scale test experiment using helium as the gas. The relevant parameters are $d = 10^{-3}$ m, $L = 10^2$ m, ρ (inlet) $= 1.4$ kg/m^3, T (inlet) $= 100$ K, $\Delta p = 2 \times 10^5$ N/m^2, $\Delta p/p$ (inlet) $= 2/3$, v_s (inlet) $= 590$ m/s, and μ (inlet) $= 9.6 \times 10^{-6}$ kg/m-s. It can easily be shown that these parameters satisfy the requirements of the LMCF ordering.

The next step is to substitute the ordering scheme into the basic model. To obtain a closed set of equations we require the following variables to the order indicated

$$\rho = \rho_0 + \ldots \tag{7a}$$

$$\mathbf{v} = (\mathbf{v}_{\perp 2} + \ldots) + (v_{z1} + \ldots)\mathbf{e}_z \tag{7b}$$

$$p = p_0 + p_2 + \ldots \tag{7c}$$

$$T = T_0 + T_1 + \ldots \tag{7d}$$

where for any quantity $Q, Q_n \sim \epsilon^n Q_0$. Observe that we require only the first nonvanishing terms for $\rho, \mathbf{v}_\perp$ and v_z but require higher order corrections for p and T. (The first order correction p_1 vanishes trivially.) The reasons for this will become apparent as the analysis progresses.

Consider first the mass equation. In the context of the LMCF expansion this equation remains unchanged as all terms are competitive. Continuing, in the perpendicular component of the momentum equation, the leading order contribution is given by

$$\nabla_\perp p_0 = 0 \tag{8a}$$

or equivalently

$$p_0 = p_0(z,t). \tag{8b}$$

To leading order the pressure is constant in the cross section. The first higher order nonvanishing contribution can be written as

$$\begin{aligned}\nabla_\perp p_2 = &-\mu\left[\nabla_\perp^2 \mathbf{v}_{\perp 2} + \frac{1}{3}\nabla_\perp(\nabla\cdot\mathbf{v})\right] + \frac{\partial\mu}{\partial z}\nabla_\perp v_{z1} \\ &+ \nabla_\perp\mu\cdot\left[\frac{2}{3}(\nabla\cdot\mathbf{v})\overleftrightarrow{\mathbf{I}} - \nabla_\perp\mathbf{v}_{\perp 2} - (\nabla_\perp\mathbf{v}_{\perp 2})^T\right].\end{aligned} \tag{9}$$

This complicated equation is required to determine the transverse dependence of the pressure.

For the parallel component of the momentum equation, only the leading order contribution is necessary

$$\frac{\partial p_0}{\partial z} = \nabla_\perp\cdot(\mu\nabla_\perp v_{z1}). \tag{10}$$

From Eqs. (9) and (10) we see that in the context of the LMCF ordering, inertia is negligible relative to viscous forces.

The next relation of interest is the energy equation. In leading order this reduces to

$$\nabla_\perp \cdot (\kappa \nabla_\perp T_0) = 0. \tag{11}$$

For tube problems the solution to Eq. (11) is $T_0 = T_0(z)$ and one must calculate to higher order to determine the transverse heat flux. In annular or slab problems with large transverse heat flow the entire solution can be obtained in leading order. In the application sections we consider the more interesting case $T_0 = T_0(z)$. For this class of problems, where the temperature is nearly constant in the cross section, we require the first higher order nonvanishing contribution, which can be written as

$$\frac{3}{2}\rho_0 R\left(\frac{\partial T_0}{\partial t} + \mathbf{v}\cdot\nabla T_0\right) + p_0 \nabla\cdot\mathbf{v} = \nabla_\perp\cdot(\kappa\nabla_\perp T_1) + \mu(\nabla_\perp v_{z1})^2. \tag{12}$$

Observe that both compression and frictional heating are included in the energy equation.

The final relation of interest is the equation of state which requires only the leading order contribution. For convenience, we summarize the LMCF equations below

$$\frac{\partial \rho}{\partial t} + \nabla\cdot\rho\mathbf{v} = 0 \tag{13}$$

$$\nabla_\perp p_2 = -\mu\left[\nabla_\perp^2\mathbf{v}_\perp + \frac{1}{3}\nabla_\perp(\nabla\cdot\mathbf{v})\right] + \frac{\partial\mu}{\partial z}\nabla_\perp v_z$$
$$+ \nabla_\perp\mu\cdot\left[\frac{2}{3}(\nabla\cdot\mathbf{v})\overleftrightarrow{\mathbf{I}} - \nabla_\perp\mathbf{v}_\perp - (\nabla_\perp\mathbf{v}_\perp)^T\right] \tag{14}$$

$$\frac{\partial p}{\partial z} = \nabla_\perp\cdot(\mu\nabla_\perp v_z) \tag{15}$$

$$\nabla_\perp\cdot(\kappa\nabla_\perp T) = 0 \tag{16}$$

$$\frac{3}{2}\rho R\left(\frac{\partial T}{\partial t} + \mathbf{v}\cdot\nabla T\right) + p\nabla\cdot\mathbf{v} = \nabla_\perp\cdot(\kappa\nabla_\perp T_1) + \mu(\nabla_\perp v_z)^2 \tag{17}$$

$$p = \rho R T \tag{18}$$

where for simplicity all subscripts have been suppressed except on p_2 and T_1. The basic unknowns in the problem are $\rho, p, T, \mathbf{v}, p_2$ and T_1. All quantities are functions of (x, y, z, t) except $p = p(z, t)$. Although there appears to be seven equations and eight unknowns,

the fact that p depends only on (z,t) allows it to be ultimately evaluated by means of an integrability condition on Eq. (17).

The specific applications discussed in the paper are concerned with steady state, two dimensional, fully developed laminar flow in a tube. Under these conditions, the LMCF model reduces to

$$\nabla \cdot \rho \mathbf{v} = 0 \tag{19}$$

$$\frac{dp}{dz} = \frac{1}{r}\frac{\partial}{\partial r}\left(r\mu\frac{\partial v_z}{\partial r}\right) \tag{20}$$

$$\frac{1}{r}\frac{\partial}{\partial r}\left(r\kappa\frac{\partial T}{\partial r}\right) = 0 \tag{21}$$

$$\frac{3}{2}\rho R\mathbf{v}\cdot\nabla T + p\nabla\cdot\mathbf{v} = \frac{1}{r}\frac{\partial}{\partial r}\left(r\kappa\frac{\partial T_1}{\partial r}\right) + \mu\left(\frac{\partial v_z}{\partial r}\right)^2 \tag{22}$$

$$p = R\rho T. \tag{23}$$

Here, $\mathbf{v} = v_r\mathbf{e}_r + v_z\mathbf{e}_z$, and ρ, T, T_1 and $\mathbf{v}$ are functions of (r,z). The pressure $p = p(z)$ is determined by means of an integrability condition on Eq. (22). The equation for p_2 is not explicitly needed for the problems under consideration. Equations (19-23) describe low Mach number compressible flow and serve as the basis for the analysis that follows.

III. Flow in a Tube

In this section the LMCF properties in a tube are investigated. The specific problem of interest assumes that a uniform (in z) heat flux q is applied along the entire length of the tube. As previously stated, the tube is sufficiently long that entrance effects can be neglected. The goals of the analysis are to calculate the flow rate as a function of applied pressure gradient and the outlet temperature as a function of q and the inlet temperature. In contrast to incompressible flow it is shown that the evaluation of the flow rate $\dot{m}$ and exit temperature T_e are coupled, with $\dot{m}$ a function of q and T_e a function of Δp. Once the solutions are obtained, a short calculation is presented giving the LMCF friction factor and Nusselt number, which are then compared to the corresponding incompressible results.

A. Analysis

The analysis proceeds as follows. Since p is only a function of z, Eq. (20) can be immediately integrated with respect to r, leading to a Poiseuille-like profile for the parallel velocity

$$v_z(r,z) = -\frac{p'b^2}{4\mu}\left(1-\frac{r^2}{b^2}\right). \tag{24}$$

Here, prime denotes d/dz, $b = d/2$ is the radius of the tube, and the no slip boundary condition $v_z(b,z) = 0$ has been applied. Note that p' is not automatically a constant as it is for incompressible flow.

Next, the expression for v_z is substituted into the mass equation, Eq. (19), which is then formally integrated to obtain an expression for v_r. Eliminating ρ by means of the equation of state leads to

$$v_r(r,z) = \frac{b^2T}{4rp}\frac{\partial}{\partial z}\left[pp'\int_0^r \frac{1}{\mu T}\left(1-\frac{r^2}{b^2}\right) r\, dr\right]. \tag{25}$$

To proceed further, we note that the solution to Eq. (21) satisfying the regularity condition at the origin is $T = T(z)$. This leads to the following simplified expression for v_r

$$v_r(r,z) = \frac{b^4T}{4rp}\left(\frac{pp'}{\mu T}\right)'\left(\frac{1}{2}\frac{r^2}{b^2}-\frac{1}{4}\frac{r^4}{b^4}\right). \tag{26}$$

The normal velocity boundary condition corresponding to a solid wall is $v_r(b,z) = 0$ implying that

$$\left(\frac{pp'}{\mu T}\right)' = 0 \tag{27}$$

and that $v_r(r,z) = 0$ everywhere. Equation (27) represents one relation between the unknowns $p(z)$ and $T(z)$. A more complicated condition, for instance corresponding to porous flow through the boundary, can be treated in a straightforward manner, but for simplicity we consider only the solid wall condition.

The final information to complete the solution results from the energy equation, Eq. (22). A short calculation yields an equation for $T_1(r,z)$

$$\frac{1}{r}\frac{\partial}{\partial r}\left(r\kappa\frac{\partial T_1}{\partial r}\right) = -\frac{b^2}{4}\left\{\left[\frac{3}{2}\frac{pp'T'}{\mu T}+p\left(\frac{p'}{\mu}\right)'\right]\left(1-\frac{r^2}{b^2}\right)+\frac{p'^2}{\mu}\frac{r^2}{b^2}\right\} \tag{28}$$

Equation (28) is solved as follows. To begin, note that for a solution for T_1 to exist, the right-hand side of Eq. (28) must satisfy an integrability condition. This condition yields a second relation between p and T and is obtained by forming $\int_0^b r\,dr$ and using the boundary condition $\kappa\partial T(b,z)/\partial r = \kappa\partial T_1(b,z)/\partial r = q$. (Here, $q > 0$ represents energy input). The integrability condition is given by

$$q = -\frac{b^3}{16}\left[\frac{3pp'T'}{2\mu T} + p\left(\frac{p'}{\mu}\right)' + \frac{p'^2}{\mu}\right]. \tag{29}$$

B. The Case μ = const.

Equations (27) and (29) can easily be solved for p and T for the case μ = const. The result is

$$p^2 = p_i^2 - (p_i^2 - p_e^2)\left[(1+Q)\frac{z}{L} - Q\frac{z^2}{L^2}\right] \tag{30}$$

$$T = T_i\left(1 + \frac{2Q}{1-Q}\frac{z}{L}\right) \tag{31}$$

where T_i is the inlet temperature, p_i is the inlet pressure, p_e is the exit pressure and

$$Q \equiv \frac{32\mu L^2 q}{5b^3(p_i^2 - p_e^2)} \tag{32}$$

is a dimensionless heat flux, normalized to the pressure drop along the tube.

The mathematical solution is completed by substituting the expressions for $p^2(z)$ and $T(z)$ into the equation for T_1, Eq. (28). This yields

$$\frac{1}{r}\frac{\partial}{\partial r}\left(r\kappa\frac{\partial T_1}{\partial r}\right) = \frac{4q}{b}\left(1 - \frac{r^2}{b^2}\right) + \frac{b^2 p'^2}{4\mu}\left(1 - \frac{2r^2}{b^2}\right) \tag{33}$$

which has as its solution

$$T_1 = \frac{bq}{\kappa}\left[\left(\frac{r^2}{b^2} - \frac{r^4}{4b^4} - \frac{3}{4}\right) + \frac{P}{Q}\left(\frac{r^2}{b^2} - \frac{r^4}{2b^4} - \frac{1}{2}\right)\right] + \tilde{T}(z). \tag{34}$$

Here P is a dimensionless function of z defined as

$$P(z) \equiv \frac{2}{5}\frac{L^2 p'^2(z)}{p_i^2 - p_e^2} \sim O(1). \tag{35}$$

Equation (34) has a homogeneous solution of the form $\tilde{T}(z)$ which cannot be determined until next order in the expansion. However, its value is not required when calculating the heat flux and heat transfer coefficient. Finally in Eq. (34), note that $\kappa = \kappa[T(z)]$ to lowest order.

C. Discussion of the Case $\mu = \text{const.}$

The LMCF solutions are now complete and can be compared with the corresponding incompressible flow solutions in terms of profiles, flow rates, temperature differences, friction factors and Nusselt numbers.

Consider first the profiles. Summarized below are the LMCF and incompressible flow profiles (including frictional heating) for p, T, and v.

Pressure Profiles

$$p = \left\{ p_i^2 - (p_i^2 - p_e^2) \left[(1-Q)\frac{z}{L} + Q\frac{z^2}{L^2} \right] \right\}^{1/2} \tag{36a}$$

$$\hat{p} = p_i - (p_i - p_e)\frac{z}{L} \tag{36b}$$

Temperature Profiles

$$T = T_i \left(1 + \frac{2Q}{1-Q}\frac{z}{L} \right) + \frac{bq}{\kappa} \left[\frac{r^2}{b^2} - \frac{r^4}{4b^4} - \frac{3}{4} + \frac{P}{Q} \left(\frac{r^2}{b^2} - \frac{r^4}{2b^4} - \frac{1}{2} \right) \right] + \tilde{T}(z) \tag{37a}$$

$$\hat{T} = T_i \left[1 + \left(\hat{Q} + \hat{P} \right) \frac{z}{L} \right] + \frac{bq}{\kappa} \left[\frac{r^2}{b^2} - \frac{r^4}{4b^4} - \frac{3}{4} + \frac{\hat{P}}{\hat{Q}} \left(\frac{r^2}{b^2} - \frac{r^4}{2b^4} - \frac{1}{2} \right) \right] + \tilde{T}(z) \tag{37b}$$

Velocity Profiles

$$v_z = \frac{b^2(p_i^2 - p_e^2)}{8\mu L}\left[\frac{1 - Q + 2Q(z/L)}{p}\right]\left(1 - \frac{r^2}{b^2}\right) \tag{38a}$$

$$\hat{v}_z = \frac{b^2(p_i - p_e)}{4\mu L}\left(1 - \frac{r^2}{b^2}\right). \tag{38b}$$

In these expressions, $\hat{}$ denotes the incompressible solution, $\hat{Q} \equiv 16\mu L^2 q/b^3 C_p \rho T_i(p_i - p_e)$, $\hat{P} \equiv (p_i - p_e)/\rho C_p T_i$, and C_p is the specific heat at constant pressure. As an example the pressure and the velocity are plotted versus z/L in Fig. 1 for $p_i/p_e = 3$ and various values of Q. There are several points to note. First, p is always greater than $\hat{p}$, implying that p' is smaller as $z \to 0$ and larger as $z \to L$. This follows because heat supplied near the midpoint of the tube ($z \sim L/2$) tends to escape towards each end. The pressure gradient resulting from the heat expansion adds to the applied pressure near the end ($z \sim L$) and subtracts near the entrance ($z \sim 0$).

Second, observe that when $Q \to 1$, then $p'(0) = 0$ and $v_z(0) = 0$. The implication is that for $Q < 1$, steady state flow solutions exist with $v_z(z) > 0$ for $0 < z < L$. For $Q > 1$, the flow reverses and there are no physical steady state solutions (e.g. T becomes negative). Consequently,

$$Q \leq 1 \tag{39a}$$

or equivalently

$$q < q_c \equiv \frac{5b^3(p_i^2 - p_e^2)}{32\mu L^2} \tag{39b}$$

is required for steady state LMCF; that is, the heat flux must be sufficiently small that the reverse pressure gradient near the inlet due to heating does not overcome the applied pressure gradient. For the small scale experiment, we find that $q_c = 16.3$ W/m^2 corresponding to a total heat input along the entire length of the tube of only 5.1 watts.

Third, the ordering $Q \sim 1$ implies that $bq/\kappa T_i \sim PrM^2 \ll 1$. Consequently, $T_1/T \ll 1$, thereby justifying the expansion technique used in the solution for T.

Finally, to leading order the LMCF profiles reduce to the incompressible solution for the case $(p_i - p_e)/p_i \ll 1$ and $Q \ll 1$. In addition, by setting $Q = 0$ and treating $(p_i - p_e)/p_i$ as a small parameter we can expand the LMCF pressure and velocity profiles. These profiles reduce exactly to those given in [7] where from the outset the case $Q = 0$, $(p_i - p_e)/p_i \ll 1$ is treated.

The next topic for discussion is the flow rate-pressure drop relation and the corresponding evaluation of the friction factor. The flow rate follows from the usual definition $\dot{m} = 2\pi \int \rho v_z r \, dr$. As expected, $\dot{m}$ is independent of z for both LMCF and incompressible flow. The values are given by

$$\dot{m} = \frac{\pi b^4 (p_i^2 - p_e^2)}{16 \mu L R T_i} - \frac{2\pi}{5} \frac{Lbq}{RT_i} \tag{40a}$$

$$\hat{\dot{m}} = \frac{\pi \rho b^4 (p_i - p_e)}{8 \mu L} \tag{40b}$$

The first terms on the right-hand side have different forms but are qualitatively similar in origin; a given pressure drop drives a flow inversely proportional to the viscous friction force. The LMCF, however, has an additional flow-reducing contribution resulting from the reverse pressure gradient due to heat flow. When $q = q_c$, the flow rate reduces to zero.

The friction factor f can be found from the usual definition [10]

$$f \frac{\overline{\rho v}_z \overline{v}_z}{4b} = -\frac{2\mu}{b} \left(\frac{\partial v_z}{\partial r} \right)_b \tag{41}$$

where $\overline{U}$ denotes $(2/b^2) \int U r \, dr$. In general f can be a function of z. For both LMCF and incompressible flow, however, f is independent of z. Interestingly, in a formal sense, the friction factors are the same for both flows, given by the well known relation

$$f = \hat{f} = 64/Re \tag{42}$$

where $Re = \overline{\rho v}_z d/\mu$ and $d = 2b$. In contrast, if one rewrites the friction factor in terms of quantities that can be measured experimentally, the expressions are quite different

$$f = \frac{10\pi^2 b^5 (p_i^2 - p_e^2)}{L\dot{m}(5RT_i\dot{m} + 2\pi Lbq)} \tag{43a}$$

$$\hat{f} = \frac{4\pi^2 b^5 \rho (p_i - p_e)}{L\hat{\dot{m}}^2} \tag{43b}$$

Observe that for LMCF, one is required to measure the inlet temperature and input heat flux, in addition to the pressure drop and flow rate to experimentally determine the friction factor.

The remaining topic of interest concerns the exit temperature and the corresponding Nusselt number. The exit temperatures follow immediately from Eq. (37) and are given by

$$T_e \approx T(L) = T_i \left[\frac{5b^3(p_i^2 - p_e^2) + 32\mu L^2 q}{5b^3(p_i^2 - p_e^2) - 32\mu L^2 q} \right] \tag{44a}$$

$$\hat{T}_e \approx \hat{T}(L) = T_i \left[1 + \frac{p_i - p_e}{\rho C T_i} + \frac{8\mu L^2 q}{b^3 \rho C T_i (p_i - p_e)} \right] \tag{44b}$$

For a fixed pressure gradient the exit temperature in an incompressible fluid increases linearly with q. For an LMCF fluid, T_e increases even faster with q and approaches infinity as $q \to q_c$. The reason is that as q increases, the flow slows down, allowing the fluid to spend more time getting heated as it moves along the tube.

The Nusselt numbers are easily evaluated from the standard definition [10]

$$Nu = \frac{d(\partial T/\partial r)_b}{(T)_b - \overline{vT}/\overline{v}} = \frac{2b(\partial T_1/\partial r)_b}{(T_1)_b - \overline{vT}_1/\overline{v}} \tag{45}$$

In general Nu is a function of z. A short calculation based on Eq. (34) yields

$$Nu = \frac{48}{11 + 6P/Q} \tag{46a}$$

$$\hat{N}u = \frac{48}{11 + 6\hat{P}/\hat{Q}} \tag{46b}$$

Although the numerical values for each case are comparable, the LMCF solution is interesting in that $Nu = Nu(z)$ because of the z dependence of P. For the incompressible case $\hat{P}/\hat{Q} = \text{const.} \ll 1$. This suggests that measurements of Nu or, equivalently the heat transfer coefficient h, from LMCF experiments cannot be made globally from the inlet and exit conditions. Instead, local measurements along the length of the tube are required. The Nu number is plotted versus z/L in Fig. 2 for $p_i/p_e = 3$ and various values of Q. Note that the value of Nu along the tube is substantially different from the corresponding incompressible limit $Nu \approx 4.364$.

As a final point, we emphasize that the concept of a steady state friction factor and heat transfer coefficient only make sense for $q < q_c$. For $q > q_c$ steady state is never achieved and f and h will in general be explicit functions of time until the flow reverses and the system depletes itself of gas.

D. The Case $\mu \neq$ const.

When μ is a function of T, the solutions of the LMCF model exhibit many similar qualitative features to the μ = const. case. However, the existence of a maximum q defining the boundary of steady state operation is somewhat more subtle. To show this, we introduce a simple model for μ and κ as follows

$$\mu = \mu_i \left(\frac{T}{T_i}\right)^{\nu} \tag{47a}$$

$$\kappa = \kappa_i \left(\frac{T}{T_i}\right)^{\nu} \tag{47b}$$

The transport coefficients are normalized to their inlet values and their variation with T is characterized by the parameter ν. For real gasses $\nu \sim 1$ (for helium used in our test experiment $\nu \approx 0.7$).

The first step in obtaining a solution is to observe from Eq. (27) that

$$\frac{pp'}{\mu T} = -c \tag{48}$$

where c is an integration constant, unknown at this point. The next step is to substitute into Eq. (29) to obtain an equation for T. A short calculation gives

$$\frac{dT}{dz} = \frac{32}{5}\frac{q}{cb^3} \tag{49}$$

The solution can be written as

$$T = T_i\left(1 + \lambda\frac{z}{L}\right) \tag{50}$$

where $\lambda = (T_e - T_i)/T_i = 32qL/5cb^3T_i$ is a more physical, but still unknown, constant, replacing c. Observe that T satisfies the inlet condition $T(0) = T_i$ and is linear in z even when $\mu = \mu(T)$.

Equation (50) is substituted back into Eq. (48). The resulting relation is easily integrated yielding the following relation for $p(z)$

$$p^2(z) = p_i^2 - (p_i^2 - p_e^2)\, Q \left\{ \frac{[1+\lambda(z/L)]^{\nu+2} - 1}{(1+\nu/2)\lambda^2} \right\} \tag{51}$$

Observe that the integration constant has been chosen so that p satisfies the inlet condition $p(0) = p_i$. The unknown constant λ, related to the exit temperature is determined by requiring $p(L) = p_e$. This gives the desired relation

$$Q = \frac{(1+\nu/2)\lambda^2}{(1+\lambda)^{\nu+2} - 1} \tag{52}$$

where, as before $Q = 32\mu_i L^2 q / 5b^3(p_i^2 - p_e^2)$. The velocity profile is again given by Eq. (24) with $\mu = \mu(T)$.

Equation (52) is plotted in Fig. 3. Shown here are curves of exit temperature difference vs. input heating power (i.e. λ vs. Q) for various ν. Note that for $\nu = 0$, corresponding to $\mu = \text{const.}$, $T_e - T_i$ is a monotonically increasing function of q as long as $q < q_c$. The condition $q = q_c$ $(Q = 1)$ forces $T_e - T_i \to \infty$ and $v_z(0) \to 0$.

However, for $\nu \neq 0$ the exit temperature is a double valued function of q. Further analysis of the time dependent one dimensional model resolves the difficulties as follows. The extremum point where $dQ/d\lambda = 0$ corresponds to a point of marginal stability. The lower branch of the curve is stable for $Q < Q_m$. The upper branch is unstable, perhaps not surprising, since in this regime an increase in heating power leads to a reduction in exit temperature.

At the point $Q = Q_m, \lambda = \lambda_m$ all the solutions are well behaved – there is no transition to flow reversal nor is the exit temperature approaching infinity. To determine the behavior for $Q > Q_m$ we have solved the nonlinear time dependent equations numerically assuming the source Q is applied at $t = 0$ and using the parameters of the test experiment. The inlet velocity $v_i \equiv \overline{v}_z(z = 0)$ is shown in Fig. 4 for two cases, one with $Q < Q_m$ and the other for $Q > Q_m$. Observe that when $Q < Q_m$, the inlet velocity evolves to a steady state value. On the other hand, for $Q > Q_m$, the system never reaches a steady state and just continues to evolve until the flow reverses. Ultimately all the gas is depleted from the system.

It is also worth pointing out that the value of Q_m is substantially reduced as ν increases. For instance, when $\nu = 1$, then $Q_m = \sqrt{3} - 3/2 = 0.23$ which is much smaller than the value $Q_m = 1$ for $\nu = 0$. Also, for $\nu = 1$ the exit temperature $T_e = (1+\sqrt{3})T_i = 2.73T_i$ representing a finite but not enormous temperature rise.

The mass flow produced by a given pressure drop is obtained by a simple calculation which shows that

$$\dot{m} = \frac{\pi b^4 (p_i^2 - p_e^2)}{8\mu_i LRT_i} \frac{Q}{\lambda} \tag{53}$$

with $\lambda(Q)$ given by Eq. (52). This relation is qualitatively similar to the $\mu = \text{const.}$ case [Eq. (40a)]. The interesting feature is that the slowest allowable mass flow rate occurs when $Q = Q_m$ and $\lambda = \lambda_m$. This follows because the ratio Q/λ is a decreasing function of Q on the stable portion of the Q vs. λ curve. Unlike the $\mu = \text{const.}$ case where $\dot{m} \to 0$ when $Q = Q_m$, in this case $\dot{m}$ achieves a finite minimum value at this point. Thus, for $\nu = 1$, steady state solutions exist only for

$$\dot{m} > \left(1 - \frac{\sqrt{3}}{2}\right) \frac{\pi b^4 (p_i^2 - p_e^2)}{8\mu_i LRT_i} \tag{54}$$

The last point of interest is to obtain the friction factor and the Nusselt number. In this case we find the friction factor [given by Eq. (42)] is no longer a constant along the tube, since $Re = Re(z)$. The first order temperature $T_1(r, z)$ and the Nusselt number can again be calculated from Eqs. (33) and (45) and are given by

$$T_1 = \frac{bq}{\kappa_i} \left(\frac{T_i}{T}\right)^\nu \left[\left(\frac{r^2}{b^2} - \frac{r^4}{4b^4} - \frac{3}{4}\right) + \left(\frac{T_i}{T}\right)^\nu \frac{P}{Q} \left(\frac{r^2}{b^2} - \frac{r^4}{2b^4} - \frac{1}{2}\right)\right] + \tilde{T}(z). \tag{55}$$

$$Nu = \frac{48}{11 + 6\,(T_i/T)^\nu\, P/Q} \tag{56}$$

where P is given by Eq. (35).

E. Turbulent Flow

The effects of turbulence can be incorporated into the model in the following simple manner. Assume that μ and κ are replaced by equivalent turbulent parameters μ_T and κ_T, which are functions of T and ρ. Using the LMCF expansion and following the solution procedure previously described, we easily obtain a set of one dimensional equations for $\rho(z), T(z), p(z), \overline{v}_z(z)$:

$$\rho\overline{v}_z = \frac{\dot{m}}{\pi b^2} = \text{const.} \tag{57}$$

$$\frac{dp}{dz} = -\frac{f\rho\overline{v}_z^2}{2d} \tag{58}$$

$$\frac{3}{2}R\rho\overline{v}_z\frac{dT}{dz} + p\frac{d\overline{v}_z}{dz} = \frac{2q}{b} - \overline{v}_z\frac{dp}{dz} \tag{59}$$

$$p = R\rho T \tag{60}$$

Here,

$$\overline{v}_z \equiv \frac{2}{b^2}\int_0^b v_z r\, dr \tag{61}$$

and μ_T is defined in terms of the friction factor by

$$\mu_T\frac{\partial v_z}{\partial r}\bigg|_b = -\frac{f\rho\overline{v}_z^2}{8} \tag{62}$$

Although there is as yet no detailed experimental verification, we shall, in analogy with incompressible fluid dynamics, assume that $f = f(Re)$ in order to develop insight into the effects of turbulence on the flow properties. Also, note that as a consequence of the simple radial boundary condition on $T(r,z)$, there is no appearance of a turbulent heat transfer coefficient (i.e. we are not solving a coupled solid-gas heat transfer problem).

The solution is obtained as follows. Using the fact that $\rho\overline{v}_z = \text{const.}$ allows us to immediately integrate Eq. (59), yielding an expression for $T(z)$ given by

$$T(z) = T_i\left(1 + \lambda\frac{z}{L}\right) \tag{63a}$$

$$\lambda = \frac{T_e - T_i}{T_i} = \left(\frac{4\pi bL}{5RT_i}\right)\frac{q}{\dot{m}} \tag{63b}$$

The temperature profile is again linear in z, irrespective of the value of f, although $\lambda = \lambda(f)$.

The expression for T is substituted into the momentum equation which can also be easily integrated leading to an expression for p that can be written as

$$p^2(z) = p_i^2 - \frac{RT_iL}{2b}\left(\frac{\dot{m}}{\pi b^2}\right)^2 \int_0^{z/L} f(1+\lambda\xi)d\xi \tag{64}$$

As before the relation between λ and Q (i.e. exit temperature and heat flux) is obtained by setting $p(L) = p_e$. In normalized form, this relationship is given by

$$\frac{R_0Q^2}{32\lambda^2}\int_0^1 f(1+\lambda\xi)d\xi = 1 \tag{65}$$

where Q has been defined in conjunction with Eq. (52) and R_0 is a dimensionless parameter related to Reynolds number, defined by

$$R_0 = \frac{b^3(p_i^2 - p_e^2)}{4\mu_i^2 RT_iL} \tag{66}$$

For the test experiment $R_0 \approx 1300$.

Equation (65) is the primary equation of interest. To proceed further it is necessary to introduce a model for f. A simple analytic expression that closely approximates $f = f(Re)$ for water [4,10] is given by

$$f = \frac{64}{Re} + \frac{0.316}{Re^{0.25}} \tag{67}$$

Here, the Reynolds number can be written as

$$Re = \frac{2\rho\bar{v}_z b}{\mu_i(T/T_i)^\nu} = \frac{R_0Q}{\lambda}\frac{1}{(1+\lambda\xi)^\nu} \tag{68}$$

The first term in Eq. (67) is the familiar laminar value while the second term represents the correction due to turbulence. If one ignores the turbulence correction and substitutes $f = 64/Re$ into Eq. (65), it can easily be shown that the resulting constraint is identical to Eq. (52).

Keeping both terms and assuming $\nu = 0.7$ for helium leads to a constraint relation of the form $G(\lambda, Q, R_0) = 0$, given by

$$0.74\,\frac{(1+\lambda)^{2.7}-1}{\lambda^2}\,Q + 4.55\times10^{-3}\,\frac{(1+\lambda)^{2.175}-1}{\lambda^{2.75}}\,R_0^{0.75}Q^{1.75} = 1 \tag{69}$$

The goal now is to examine Eq. (69) to determine whether or not the addition of turbulence alters the laminar theory conclusions regarding the existence of a maximum q and a minimum $\dot{m}$ for steady state solutions.

This basic question is answered in Fig. 5 where we have plotted curves of λ vs. Q for various R_0. Observe that the qualitative nature of the curves remains unchanged as the turbulence (i.e. R_0) increases. As $R_0 \to 0$ the laminar result is recovered. For large R_0 the maximum normalized heat flux decreases with R_0 while the exit temperature increases. Illustrated in Fig. 6 are curves of the maximum Q and the corresponding value of exit temperature (λ_m) vs. R_0. Analytic expressions are easily obtained in the limit of small and large R_0 and are given by

$$\left.\begin{aligned} Q_m &= 0.297 \\ \lambda_m &= 2.50 \end{aligned}\right\} R_0 \to 0$$

$$\left.\begin{aligned} Q_m &= 7.33/R_0^{0.29} \\ \lambda_m &= 0.032 R_0^{0.42} \end{aligned}\right\} R_0 \to \infty \tag{70}$$

To understand physically the influence of turbulence, it is helpful to replot the results of Fig. 6 in unnormalized form. Thus, using the parameters for our test experiment and by varying $\Delta p \equiv p_e - p_i$, we plot in Fig. 7 the maximum q, corresponding $\dot{m}$, and corresponding ΔT vs. pressure drop. The curves labeled turbulent include the turbulent corrections to f while the curves labeled laminar are for the purely laminar case. As expected, when Δp increases the maximum allowable heat that can be removed in steady state also increases. However, the value of q with turbulence does not increase as rapidly as in the laminar case. The reason is that as Δp increases, the flow velocities increase, extending operation more and more into the turbulent regime. As the turbulence develops (i.e. R_0 increases) the friction factor, while decreasing with R_0, nevertheless increases with respect to the purely laminar value. This relative increase in f slows the flow rate, allowing each fluid element to receive more heat as it spends more time passing through the tube. It therefore requires a smaller value of q than in the laminar case to reach the critical point where steady state solutions no longer exist.

Consistent with this insight is the fact that the exit temperature increases relative to its laminar value, because of the additional time spent traversing the tube. Similarly, the relatively reduced flow rate due to turbulent friction reduces the minimum value of $\dot{m}$ required for steady state solutions.

The basic conclusion is that turbulence introduces important quantitative changes in LMCF properties but does not change the qualitative behavior. Specifically, for steady state flow the applied heat flux must lie below a critical value.

IV. Conclusions

We have investigated the basic properties of a relatively uncommon regime of fluid dynamics, low Mach number compressible flow. This regime, which is of importance in the cooling of large scale superconducting magnets, is characterized by an enormous aspect ratio $L/d \sim 10^6$. The consequence is that friction dominates inertia, leading to highly subsonic flows, even though finite pressure, temperature, and density gradients are required because of the exceptionally long lengths involved. Many features of the flow are qualitatively similar, although quantitatively different from incompressible flows. Perhaps the most surprising result is that steady state solutions exist only below a critical value of heat input. Above this value the compressibility leads to a flow reversal against the applied pressure gradient causing the gas to flow out of both the inlet and outlet, thereby depleting the coolant. The existence of a maximum heat input and a corresponding minimum flow rate are found under both laminar and turbulent conditions. Parameters have been given for a simple, small scale experiment, that could test several of the conclusions of the theory and we intend to do so in the future.

References

[1] Shajii, A. & Freidberg, J. P. 1994 *J. Appl. Phys.* **76**, 3149.

[2] Shajii, A. & Freidberg, J. P. 1994 *J. Appl. Phys.* **76**, 3159.

[3] Thome, R. J., 1994 *IEEE Trans. Mag.* **30**, 4, 1595-1601.

[4] White, F. M. 1986 *Fluid Mechanics*, McGraw-Hill.

[5] Kaviany, M. 1991 *Principles of Heat Transfer in Porous Media*, Springer-Verlog.

[6] Zanotti, F. & Carbonell, R. G. 1984 *Chem. Engng Sci.* **39**, 2, 299-311.

[7] Prud'homme, R. K., Chapman, T. W., & Bowen, J. R., 1986 *Appl. Sci. Res.* **43**, 67.

[8] Prins, H. J., 1991 *The Optimal Model for a Non-Newtonian Compressible Gas*, Rep. Fac. of Techn. Math. & Informatics., Delft Univ. of Technol.

[9] Van Den Berg, H. R., Ten Seldam, C. A., & Van Der Gulik, P. S., 1993 *J. Fluid Mech.* **246**, 1.

[10] Bird, R. B., Stewart, W. E., Lightfoot, E. N., 1960 *Transport Phenomena*, John Wiley & Sons.

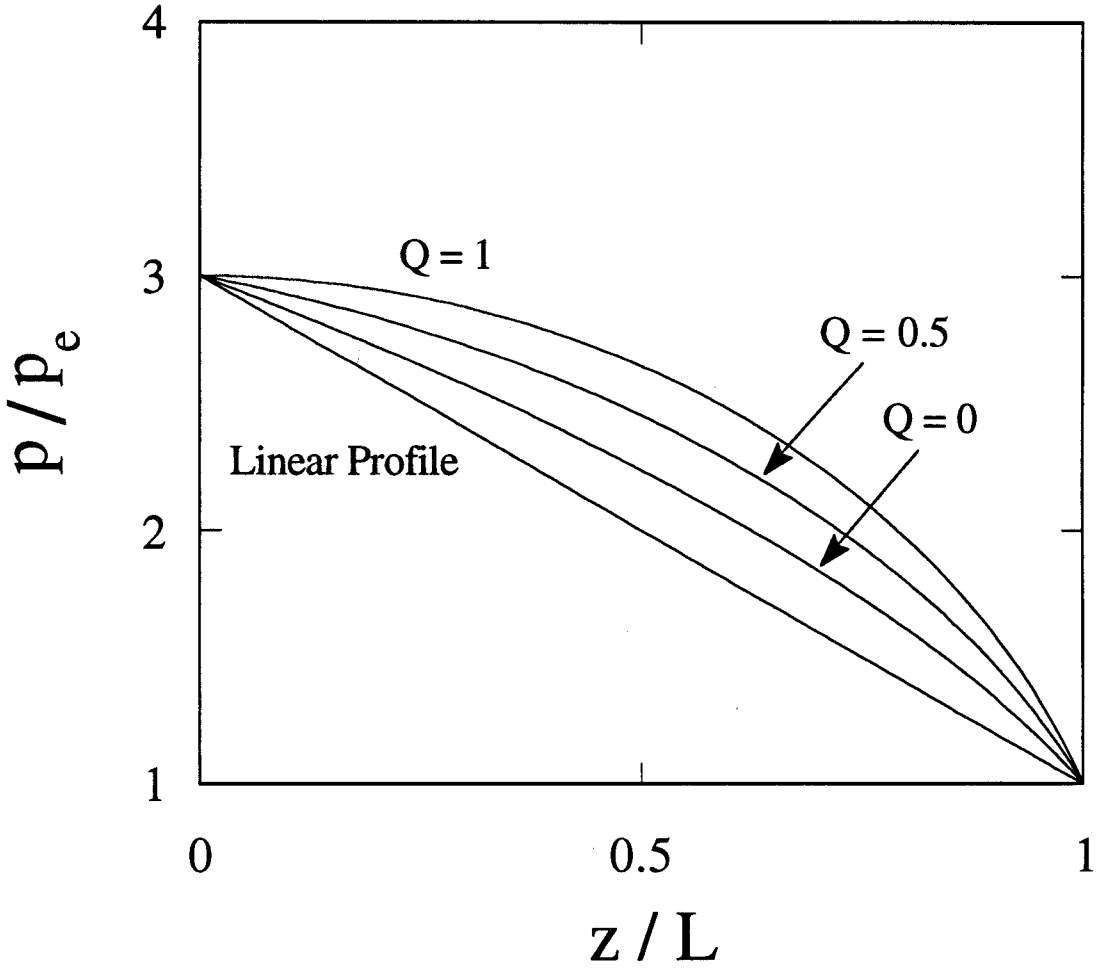

Figure 1a: Helium pressure profile along the tube given by Eq. (36a).

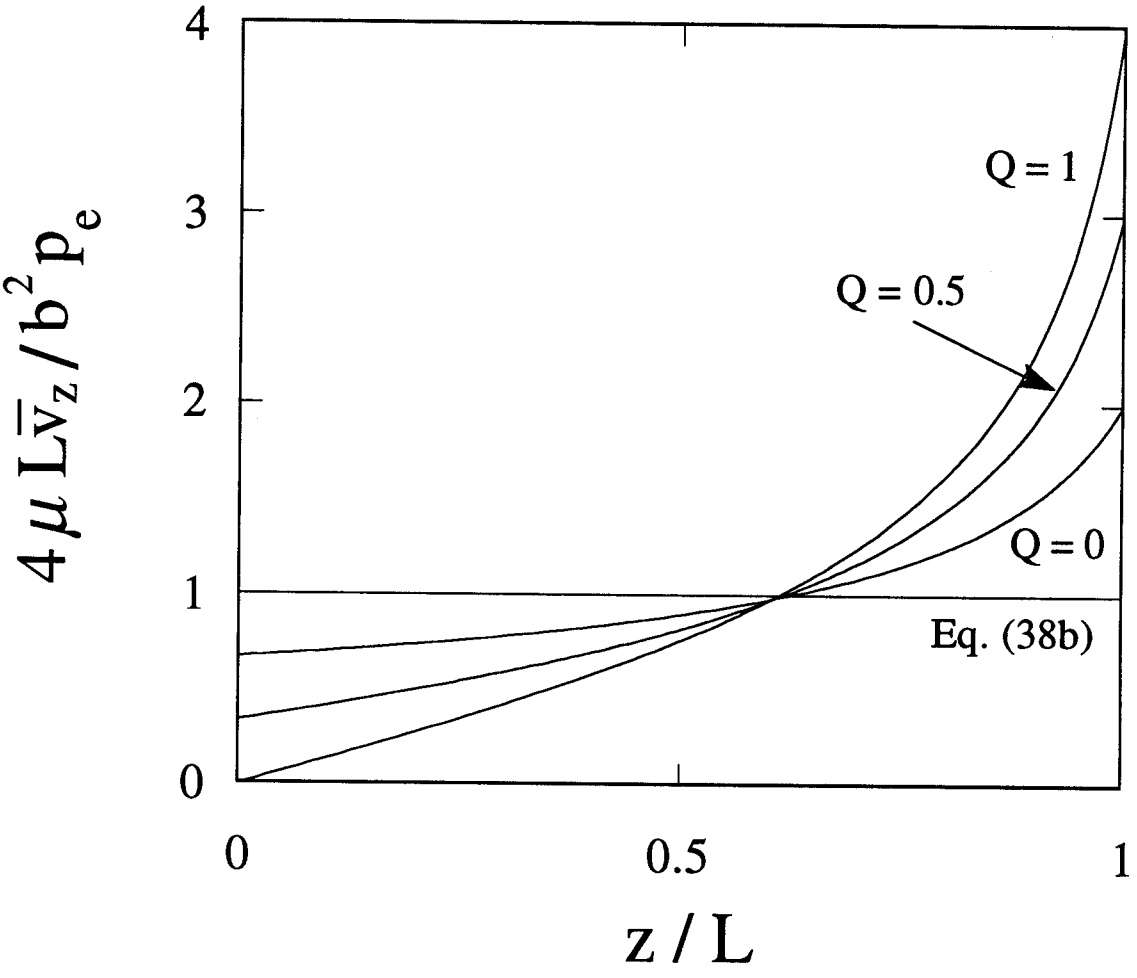

Figure 1b: Helium velocity profile along the tube given by Eq. (38a).

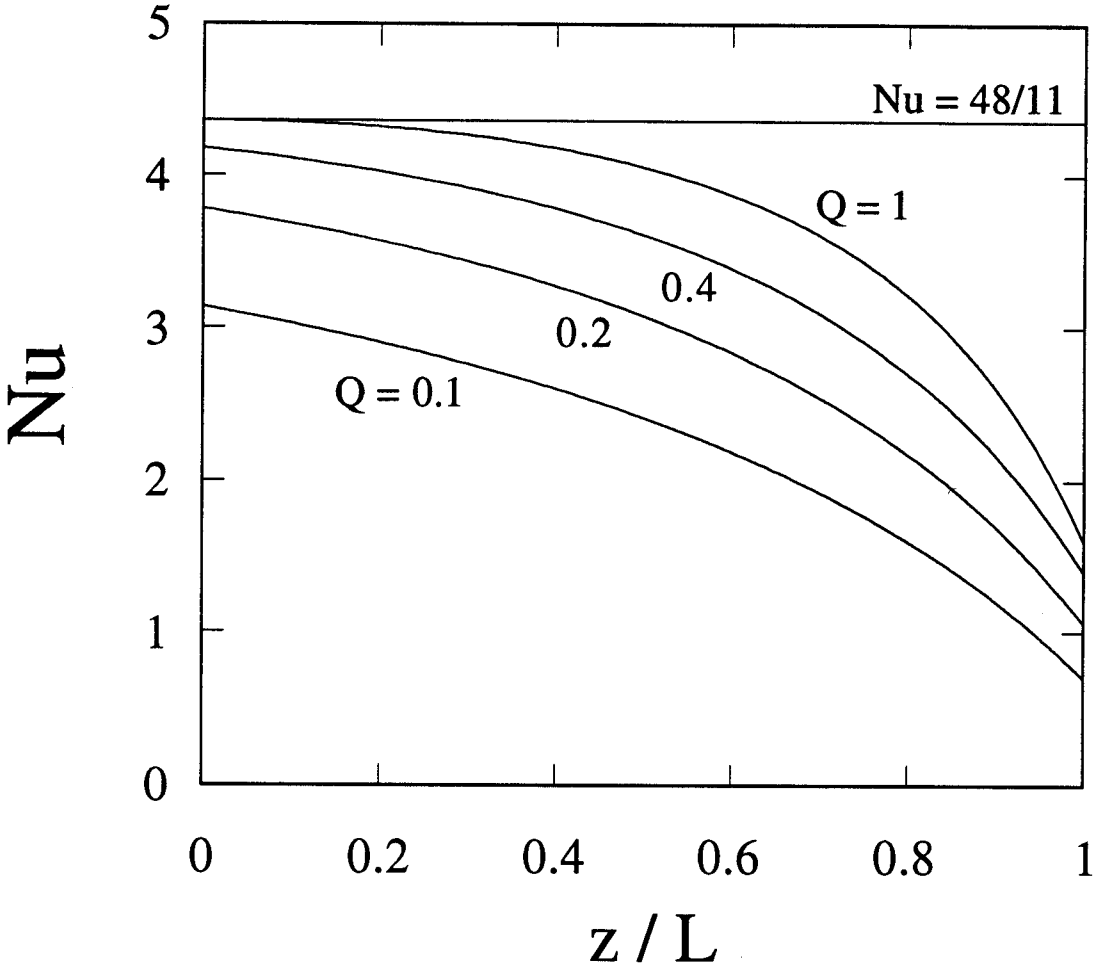

Figure 2: Nusselt number along the tube given by Eq. (46a).

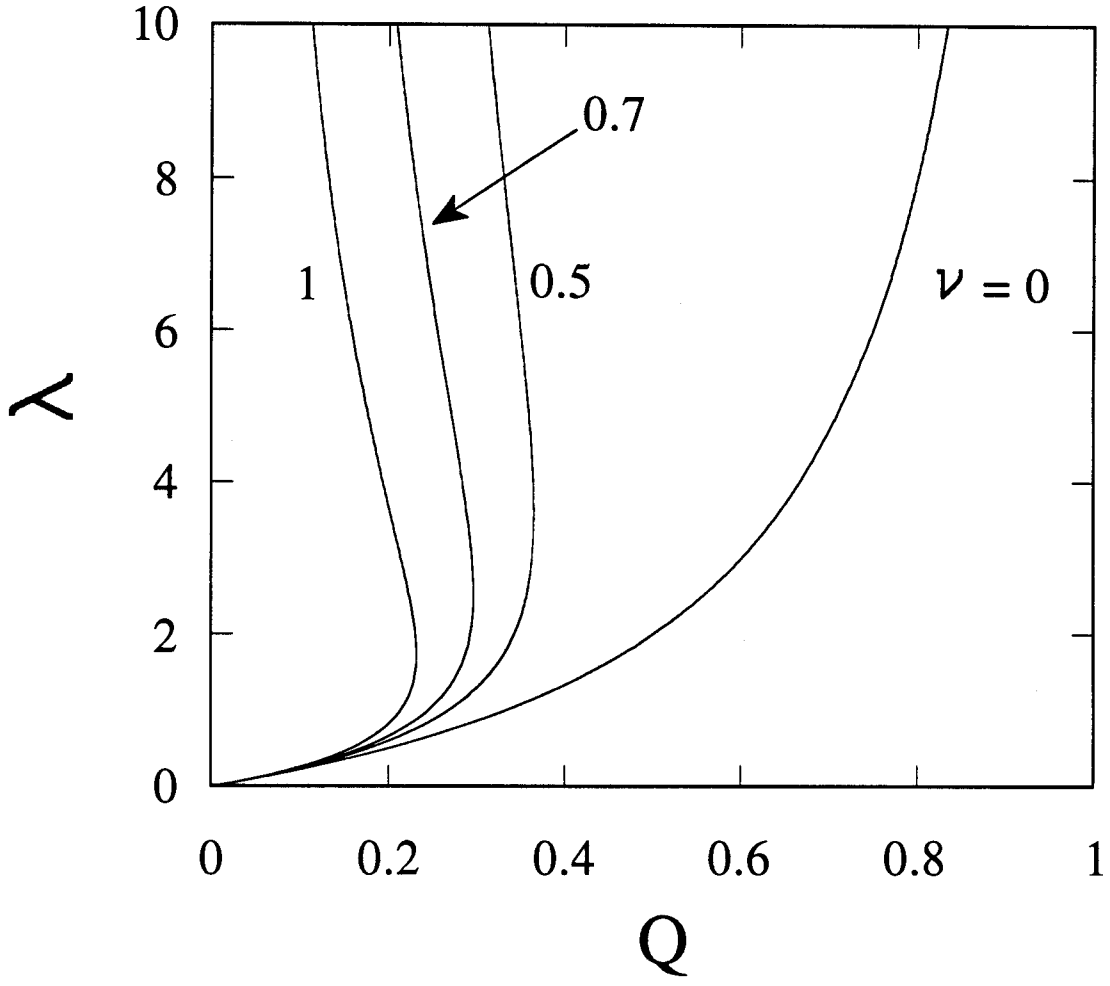

Figure 3: Curves of λ versus Q given by Eq. (52).

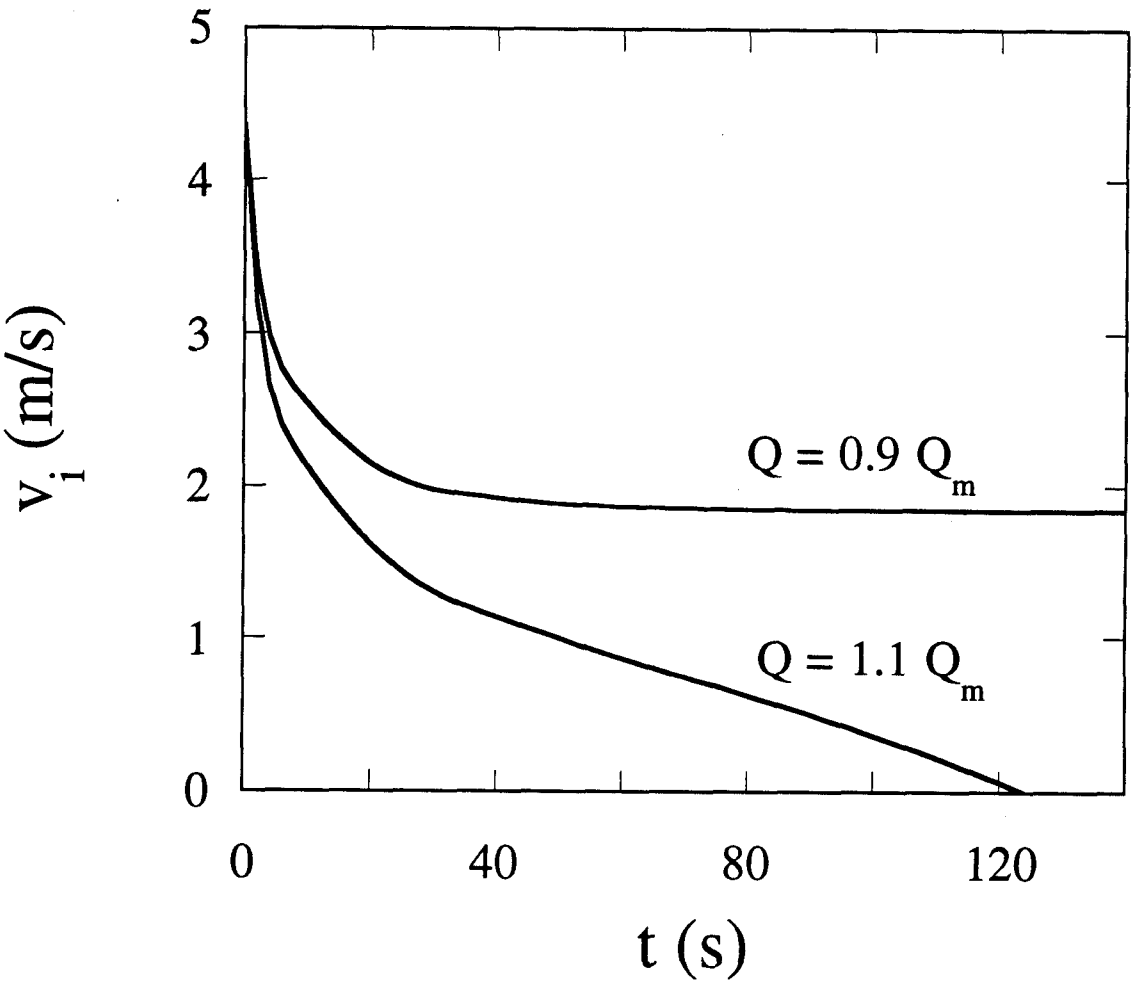

Figure 4: Time evolution of the inlet helium velocity for two different values of Q using the parameters of the test experiment.

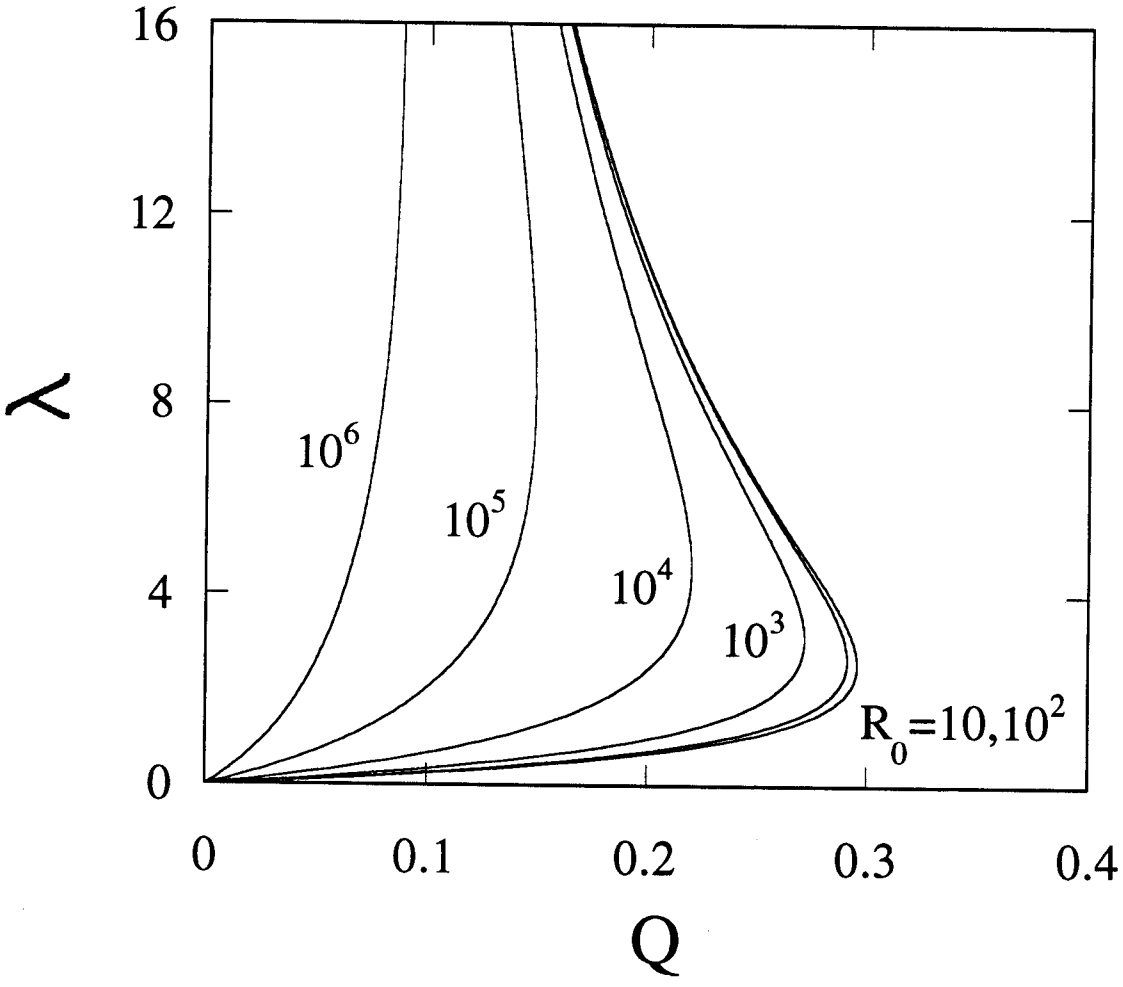

Figure 5: Curves of λ versus Q given by Eq. (69).

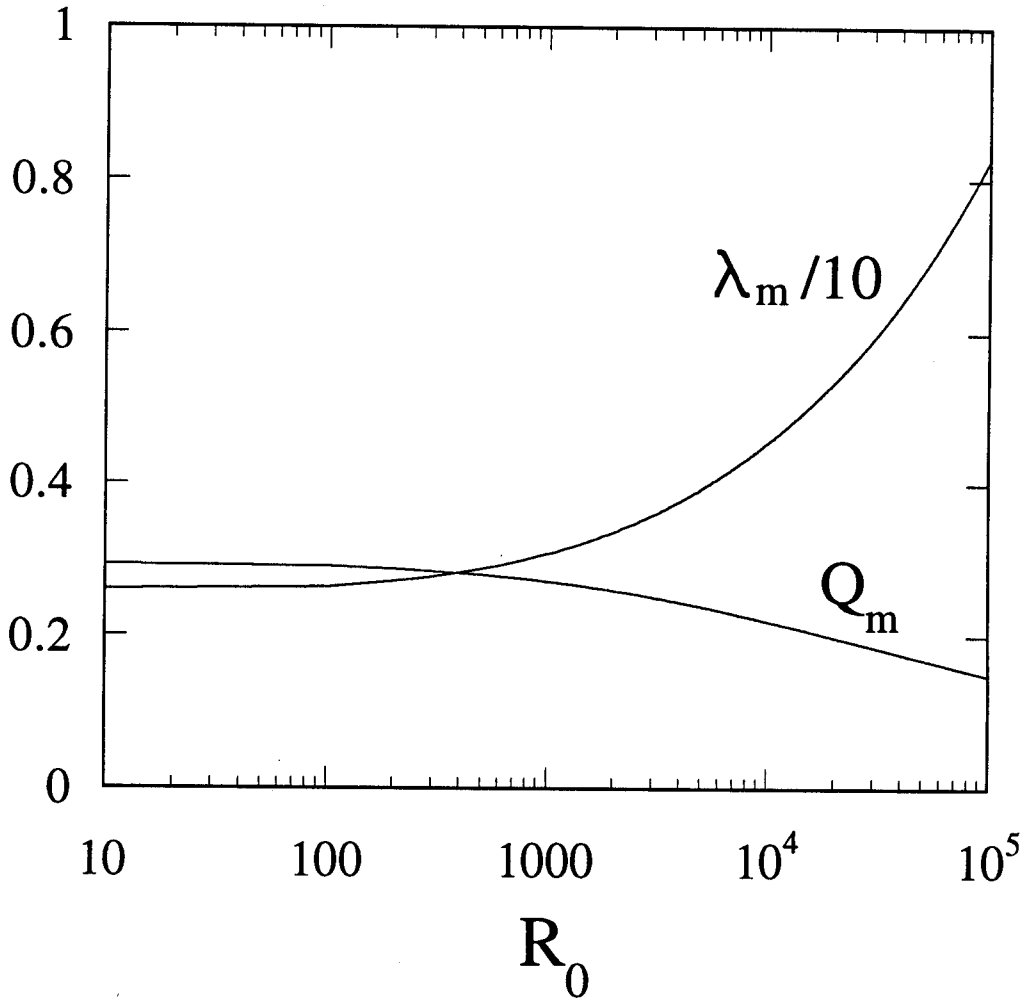

Figure 6: Dependence of λ_m and Q_m on R_0 obtained from Eq. (69).

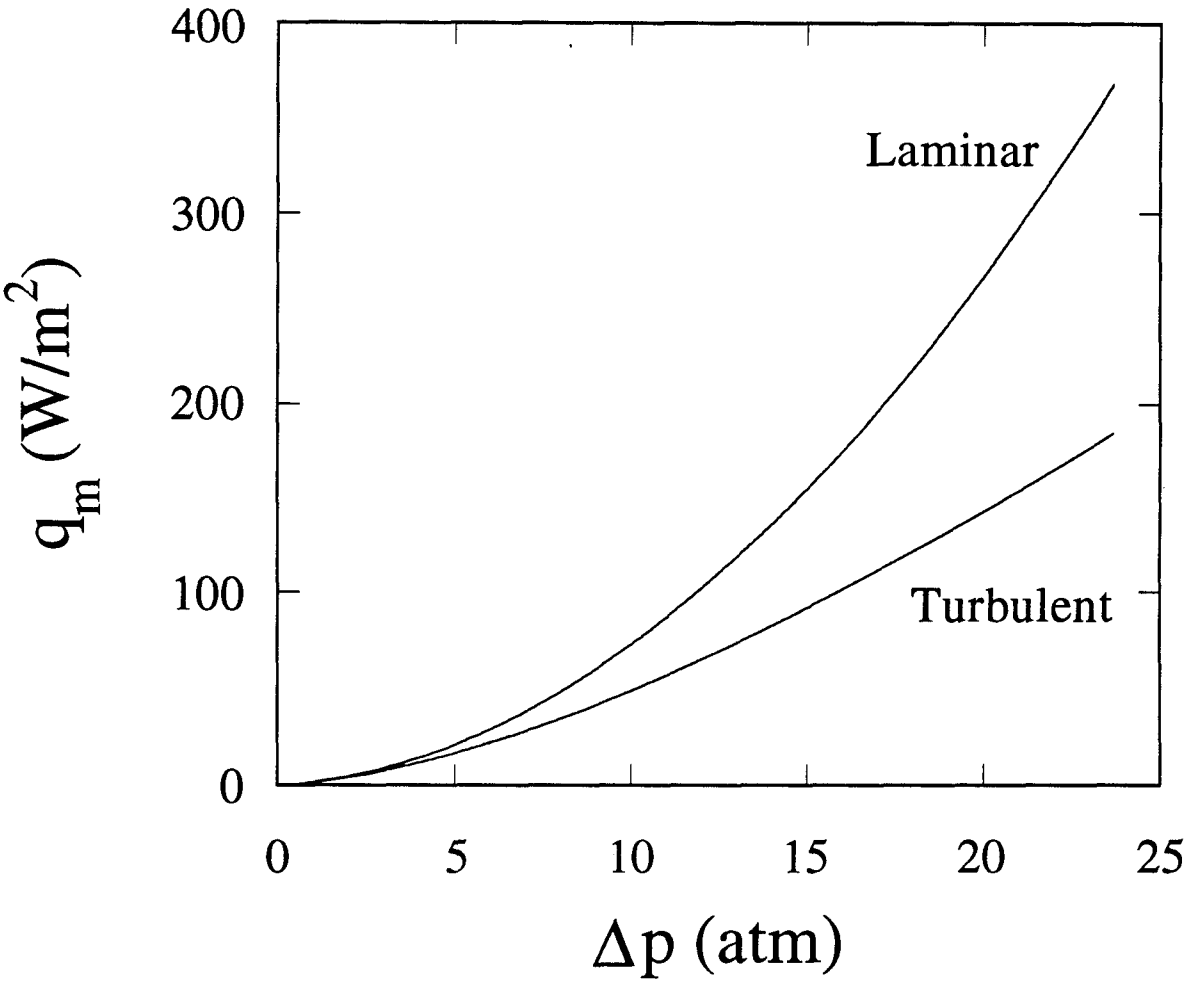

Figure 7a: Maximum allowable heat flux versus the pressure drop using the parameters of the test experiment.

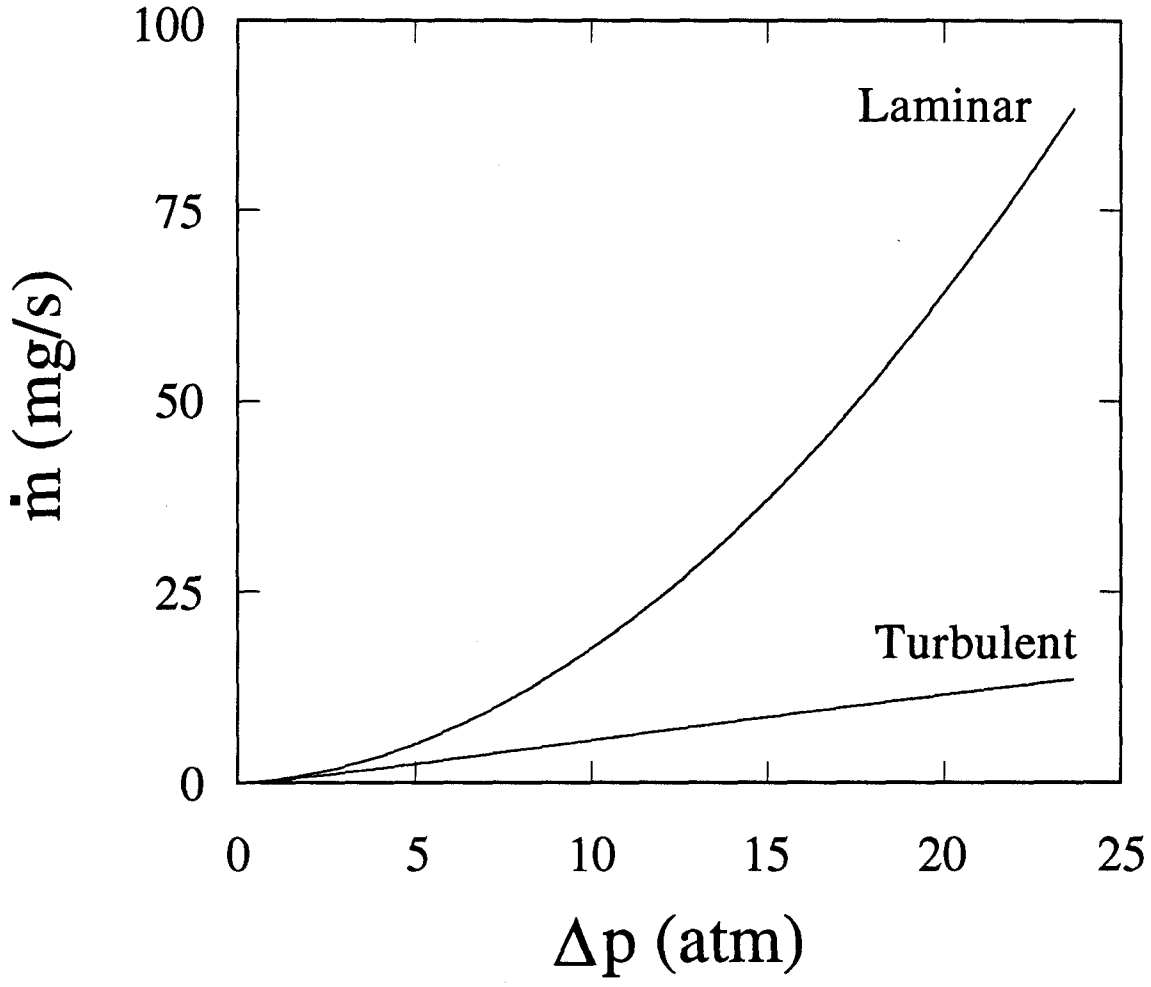

Figure 7b: Corresponding mass flow rate versus the pressure drop using the parameters of the test experiment and $q = q_m$. Note that this is the minimum obtainable $\dot{m}$.

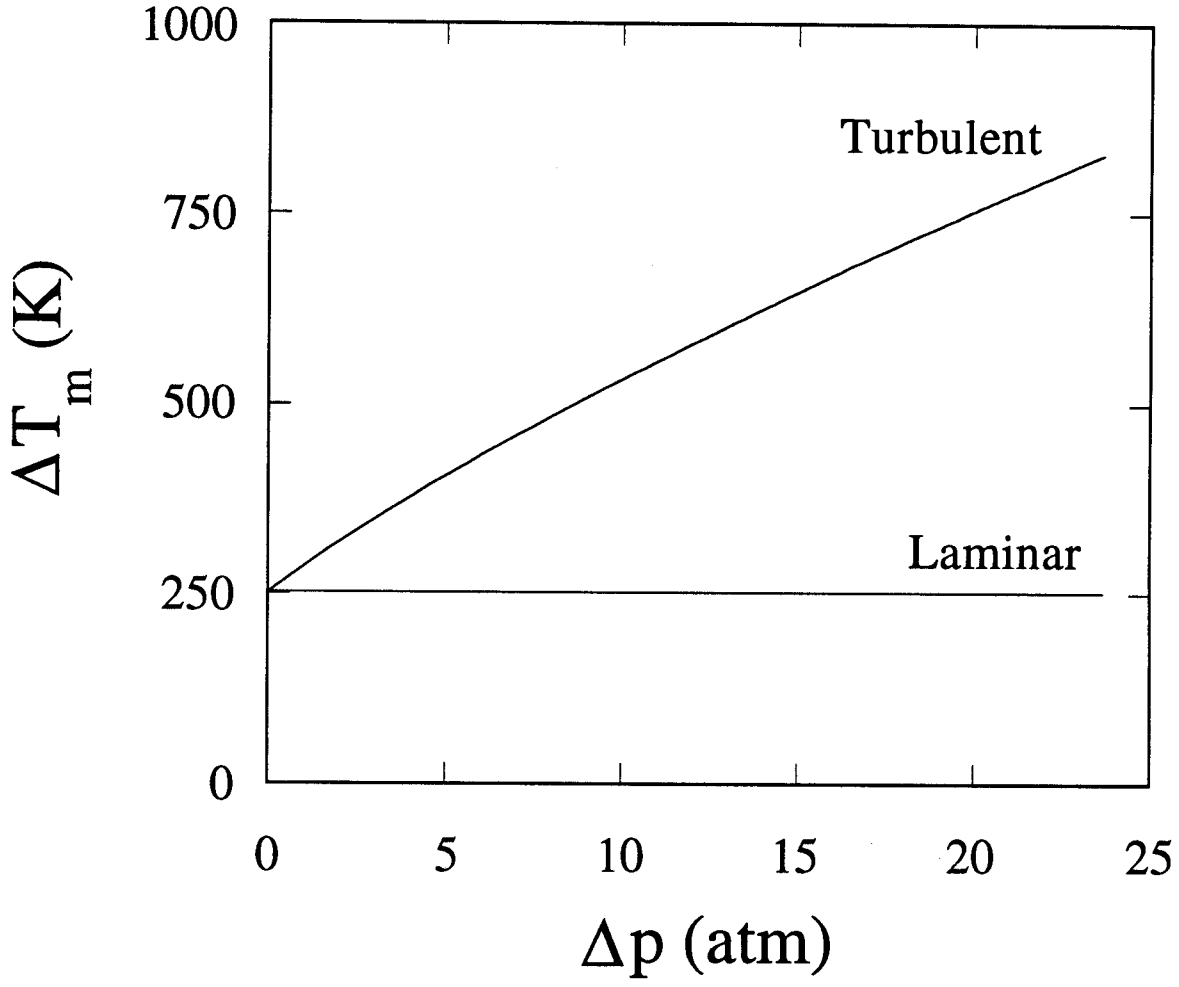

Figure 7c: Corresponding temperature rise versus the pressure drop using the parameters of the test experiment and $q = q_m$.